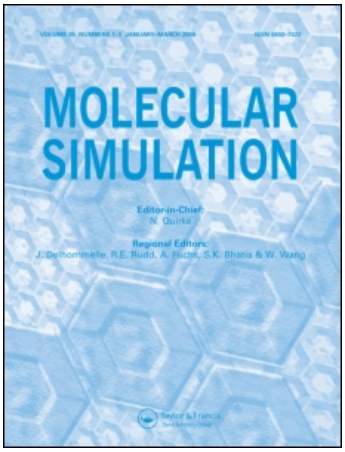

Molecular Simulation
Publication details, including instructions for authors and subscription information:
http://www.informaworld.com/smpp/title~content=t713644482

Estimating the conductivity of a nanoconfined liquid subjected to an experimentally accessible external field

Caroline Desgranges[a]; Jerome Delhommelle[a]
[a] Department of Chemical Engineering, University of South Carolina, Columbia, SC, USA

To cite this Article Desgranges, Caroline and Delhommelle, Jerome(2008) 'Estimating the conductivity of a nanoconfined liquid subjected to an experimentally accessible external field', Molecular Simulation, 34: 2, 177 — 181
To link to this Article: DOI: 10.1080/08927020801930604
URL: http://dx.doi.org/10.1080/08927020801930604

Molecular Simulation
Vol. 34, No. 2, February 2008, 177–181

Taylor & Francis
Taylor & Francis Group

Estimating the conductivity of a nanoconfined liquid subjected to an experimentally accessible external field

Caroline Desgranges* and Jerome Delhommelle

Department of Chemical Engineering, University of South Carolina, Columbia, SC, USA

(Received 27 December 2007; final version received 19 January 2008)

Using the transient-time correlation function formalism, we show how nonequilibrium molecular dynamics (NEMD) simulations can be extended to study the conductivity of a model liquid confined in a slit nanopore and subjected to an arbitrarily low (and realistic) field. This is a definite improvement over conventional NEMD methods, which are restricted to fields several orders of magnitude stronger than those accessible by experiment. Our results provide a full picture of the dependence of conductivity on the applied field in slit nanopores.

Keywords: conductivity; nanopore; nonequilibrium molecular dynamics; transient-time correlation function formalism

1. Introduction

Recent efforts in our group have focused on addressing the inability of conventional nonequilibrium molecular dynamics (NEMD) methods to study the response of a liquid subjected to experimentally accessible fields. Conventional NEMD methods only allow us to study systems subjected to very strong fields, typically of the order of $10^9\,\mathrm{V\,m^{-1}}$ [1,2], i.e. several orders of magnitude larger than the experimentally accessible rates. Conventional NEMD methods therefore only give access to the response of the fluid under far-from-equilibrium conditions. The limitation to very strong fields arises from the fact that, in conventional NEMD simulations, properties are averaged over the steady state. For strong fields, the signal-to-noise ratio is large: meaningful and reliable steady-state averages may be evaluated. On the other hand, for weak fields, the signal-to-noise ratio is very small: the steady-state response becomes very noisy and the steady-state averages are essentially impossible to analyse. This prevents conventional NEMD methods from accessing the nonequilibrium response of the system for realistic values of the field.

To address this issue, we consider the transient time correlation function (TTCF) formalism [3–6]. The TTCF formalism is essentially a nonlinear generalisation of the Green–Kubo relations. Though this formalism is fairly general, applications of the TTCF approach have been restricted so far to the determination of the viscosity of simple fluids at low shear rates [7–10], to simple liquids undergoing elongational flow [11] and, more recently, to determine the viscosity of decane [12] and of liquid metals [13] (conventional NEMD methods only allow to study the response at shear rates of the order of e.g. $10^{10}\,\mathrm{s^{-1}}$ for a liquid metal [14], which are several orders of magnitude larger than those accessible by experiments) and the electric conductivity of molten sodium chloride [15]. In this work, we show how the TTCF approach can be applied to determine the conductivity of a fluid confined in a slit nanopore and subjected to a realistic field. The paper is organised as follows. In the next section, we present the model used in this work and give the equations of motion followed by the system. We then explain how we apply the TTCF formalism to determine the conductivity and briefly discuss some technical details. We finally present and discuss the main results obtained in this work.

2. Microscopic model

From a practical point of view, applying the TTCF method consists of monitoring the response of the system over a large number of nonequilibrium trajectories. For that purpose, we generate many equilibrium configurations during the course of a long equilibrium trajectory (governed by Newton's equations of motion). Each of these configurations is the starting point for a nonequilibrium trajectory. The nonequilibrium trajectory is generated by subjecting the fluid to a colour field $\vec{E}$ along the x direction. During both the equilibrium and nonequilibrium trajectories, the temperature of the system is fixed by adding a thermostatting term to the equations of motion. Using a thermostat for the whole confined fluid relies on the assumption that, when the confined fluid is subjected to an external field, no

*Corresponding author. Email: desgrang@engr.sc.edu

ISSN 0892-7022 print/ISSN 1029-0435 online

DOI: 10.1080/08927020801930604
http://www.informaworld.com

significant temperature gradient develops across the confined fluid. The essentially flat temperature profiles observed in previous work [16–18] support this approximation. We expect even flatter temperature profiles for the very weak fields studied in this work with the TTCF approach. The choice of a specific thermostatting method may have a significant effect on the results obtained during the nonequilibrium trajectories [19–24]. Most thermostats fix the value taken by a kinetic expression for the temperature defined from an *ad hoc* version of the equipartition theorem [1,2]. In this expression, the temperature is evaluated from the streaming kinetic energy, i.e. the kinetic energy relative to the flow of each species. Any inaccuracy in the determination of the flow velocities may result in inaccuracies in the calculated current and conductivity. Recent work has shown that this problem can be circumvented by using a configurational thermostat [25–30] based on a purely configurational expression for the temperature [31,32].

The equations of motion for the nonequilibrium trajectories are defined as follows

$$\begin{aligned} \dot{\vec{r}}_i &= \tfrac{\vec{p}_i}{m} - \eta \nabla_i \Phi \\ \dot{\vec{p}}_i &= -\nabla_i \Phi + z_i \vec{E} \\ \dot{\eta} &= \tfrac{1}{Q_\eta}\left(\textstyle\sum_{i=1}^{N} (\nabla_i \Phi)^2 - k_B T \sum_{i=1}^{N} \nabla_i^2 \Phi\right) \end{aligned} \tag{1}$$

in which $\vec{r}_i$, $\vec{p}_i$, m and z_i denote the position, momentum, mass and charge of particle i, $\vec{E}$ the colour field (colinear to the x axis), Φ the potential energy of the system, k_B Boltzmann's constant, T the target value for the temperature and η an additional dynamical variable which plays the role of a friction coefficient. Q_η can be thought of as the mass associated with the heat bath. The equations of motion for the equilibrium trajectories can be recovered by simply setting $\vec{E} = \vec{0}$. This thermostat fixes the configurational temperature T_{conf} defined as

$$k_B T_{conf} = \left\langle \sum_{i=1}^{N} (\nabla_i \Phi)^2 \right\rangle \Big/ \left\langle \sum_{i=1}^{N} \nabla_i^2 \Phi \right\rangle$$

to the target value. As shown by Braga and Travis [30], these equations of motion generate the canonical distribution.

3. Estimating the colour conductivity using TTCF

We now briefly outline the general derivation proposed by Evans and Morriss [6] to show how it can be applied to a fluid following the equations of motion given by Equation (1). Let us consider a phase variable $B(\vec{\Gamma})$, where $\vec{\Gamma}$ denotes a phase space point. In the Heisenberg representation, the average of B at time t is $\langle B(t)\rangle = \int d\vec{\Gamma} f(0) B(\vec{\Gamma}; t)$, where $f(0)$ is the initial distribution function.

If we differentiate this expression with respect to time, we obtain, for time-independent external fields

$$\frac{d\langle B(t)\rangle}{dt} = \int d\vec{\Gamma} f(0) \frac{d\vec{\Gamma}}{dt} \cdot \frac{\partial B(t)}{\partial \vec{\Gamma}}. \tag{2}$$

By integrating by parts and realising that the boundary term vanishes in periodic systems [6], we see that

$$\frac{d\langle B(t)\rangle}{dt} = -\int d\vec{\Gamma} B(t) \frac{\partial}{\partial \vec{\Gamma}} \cdot \frac{d\vec{\Gamma}}{dt} f(0). \tag{3}$$

Finally, integrating with respect to time, we obtain the nonlinear nonequilibrium response

$$\langle B(t)\rangle = \langle B(0)\rangle - \int_0^t ds \int d\vec{\Gamma} B(s) \frac{\partial}{\partial \vec{\Gamma}} \cdot \frac{d\vec{\Gamma}}{dt} f(0). \tag{4}$$

If the initial distribution is canonical and if the dynamics of the system follows Equation (1), then, to the first order [6],

$$\begin{aligned} \frac{\partial}{\partial \vec{\Gamma}} \cdot \left(f(0) \frac{d\vec{\Gamma}}{dt} \right) &= f(0) \cdot \left[\frac{\partial \dot{\vec{\Gamma}}}{\partial \vec{\Gamma}} + \dot{\vec{\Gamma}} \cdot \frac{\partial}{\partial \vec{\Gamma}} \left(\frac{-H_0(\vec{\Gamma})}{k_B T} \right) \right] \\ &= f(0) \left(-\frac{V}{k_B T} \sum_{i=1}^{N} \frac{\vec{E}.\vec{p}_i}{m} \right) \end{aligned} \tag{5}$$

where

$$H_0 = \sum_{i=1}^{N} \vec{p}_i^{\,2}/2m + \Phi + Q_\eta \eta^2/2$$

is the Hamiltonian of the extended system.

Since $\vec{E}$ is $\ddot{y}$ colinear to the x axis, we define the colour current along the x axis as

$$J_x = \sum_{i=1}^{N} z_i \vec{p}_i / mV$$

where V is the volume accessible to the confined fluid. The average of B at time t is equal to

$$\langle B(t)\rangle = \langle B(0)\rangle + \frac{VE}{k_B T} \int_0^t \langle B(s) \cdot J_x(0)\rangle ds. \tag{6}$$

If we choose $B(t) = J_x(t)$, the equilibrium average $\langle J_x(0)\rangle$ is equal to 0 and we obtain the following

expression for $\langle J_x(t)\rangle$

$$\langle J_x(t)\rangle = \frac{VE}{k_B T}\int_0^t \langle J_x(s)\cdot J_x(0)\rangle \mathrm{d}s. \quad (7)$$

It is then straightforward to evaluate the colour conductivity according to

$$\langle \sigma(t)\rangle = \frac{V}{k_B T}\int_0^t \langle J_x(s)\cdot J_x(0)\rangle \mathrm{d}s. \quad (8)$$

4. Simulation details

The interactions between particles were modelled using the Weeks–Chandler–Anderson modification of the Lennard-Jones potential (if r is the distance between two particles, $\phi(r) = -4\varepsilon[(\sigma/r)^6 - (\sigma/r)^{12}] + \varepsilon$ for $r \leq 2^{1/6}\sigma$ and 0 otherwise). The two types of particle only differ by the way they couple to the colour field (half of the particle is assigned a charge $z_i = 1$ while the other half is assigned $z_i = -1$). In other words, there is no coulombic interaction between particles. Throughout this work, we use a reduced system of units [33] in which the units of length, mass and energy are σ, m and ϵ. We carried out simulations of the bulk as well as of the confined fluid. We choose to confine the fluid between two walls, separated from each other by a distance D, perpendicular to the y axis. The interaction between the particles and the confining wall is defined as $\phi_{wf}(y) = \varepsilon[(\sigma/(D/2 - y)^{12}) + (\sigma/(D/2 + y)^{12})]$. All simulations for the bulk and the confined systems were carried out at constant number density $n = 0.84$ and constant temperature $T = 0.75$. We used systems of $N = 256$ particles for simulations of the bulk and of the narrower pores ($D = 4$, 5 and 7.5) and $N = 350$ particles for the larger pore ($D = 10$). As always, there is some ambiguity in defining the effective radius and thus the effective volume for the confined system. To determine the effective volume, we ran an equilibrium molecular dynamics simulation for each system and determined the maximum value reached by $|y_i|$, where i is a fluid particle, during the course of the simulation. This allows to define the effective pore width by $D_{eff} = D - 1.74$. We integrate the equations of motion with a Runge–Kutta integrator and a time step of 2×10^{-3}. The parameter for the configurational thermostat Q_η is set to 5×10^5 as in [30]. Periodic boundary conditions are applied to the system in the three directions of space for the simulations of the bulk and in the x direction only for the simulations of the confined fluid. Each system was started off by inserting the particles at random positions within the desired volume. The systems were first equilibrated for 10^6 timesteps. During subsequent simulation runs, we selected 10,000 equilibrium configurations for each system at intervals of 2–3 time units. From each of these configurations, we can define three other equilibrium configurations: (i) by reversing the sign of the momenta of all particles (also termed as time-reversal mapping [6]), (ii) by mirror symmetry (reversing the sign of x and p_x for all particles) and (iii) by applying both the time-reversal mapping and the mirror symmetry. The 40,000 configurations so obtained were the starting points for the nonequilibrium trajectories. In addition to being more efficient, this procedure also ensured that the $\langle J_x(0)\rangle$ was exactly zero.

5. Results and discussion

We present in Figure 1 the TTCF results obtained for the colour current (using Equation (7)) when the fluid is confined in a slit pore with a pore width of $D = 4$. As shown in Figure 1, the TTCF approach allows us to obtain reliable estimates of the colour current for a confined fluid, both in the transient regime and in the steady state, over the whole range of fields we studied i.e. from 10^{-9} to 0.1. We plot in Figure 2 the TTCF estimates of the colour conductivity (using Equation (8)) for a fluid confined in a slit pore with a pore width of $D = 4$. For a high value of the field, a direct steady-state average should coincide with the TTCF estimate. This is because (i) the TTCF formalism gives an exact relation between the nonlinear steady-state response and the TTCF and (ii) for a strong enough field, the signal-to-noise ratio is large enough for steady-state averages to be measured. The direct steady-state average can be measured during

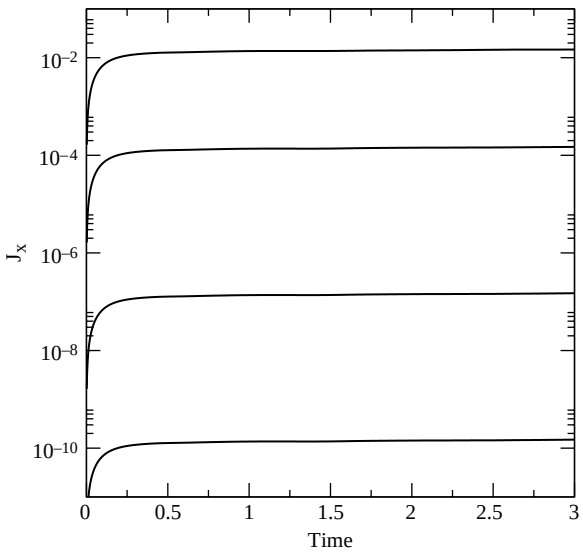

Figure 1. $D = 4$. Colour current against the colour field for an applied field of 0.1, 10^{-3}, 10^{-6} and 10^{-9} (from top to bottom).

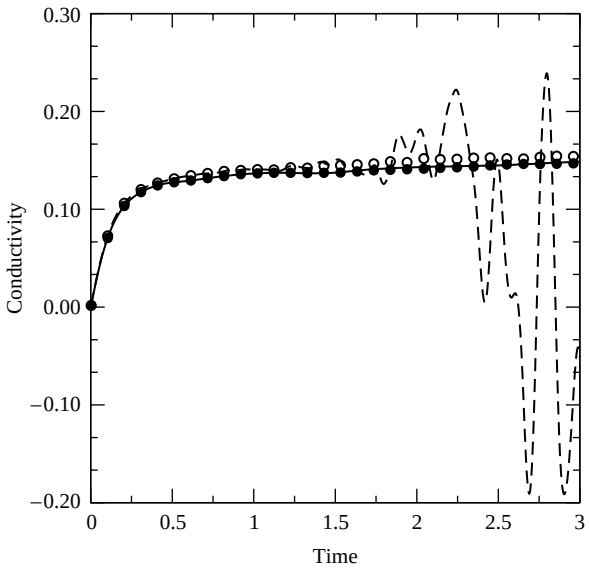

Figure 2. $D = 4$. Colour current against the colour field for an applied field of 0.1 (open circles, direct average; filled circles, TTCF estimate) and 10^{-6} (dashed line, direct average and solid line, TTCF estimate).

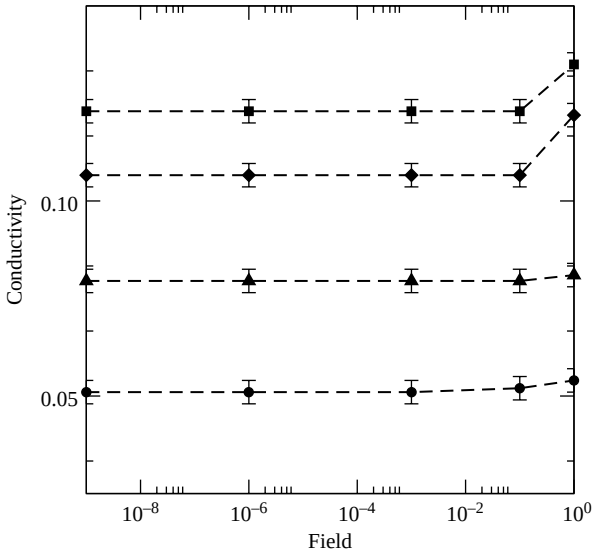

Figure 3. Colour conductivity as a function of the applied colour field: bulk (circles) and slit nanopores with a pore width of 4 (squares), 5 (diamonds) and 7.5 (triangles).

the course of the NEMD simulations as

$$\langle J_x(t)\rangle = \frac{\sum_{i=1}^{N} J_{x,i}(t)}{N_t} \tag{9}$$

where $N_t = 40{,}000$ is the number of nonequilibrium trajectories considered. As shown in Figure 2 for a field of 0.1, the direct steady-state average and the TTCF estimate for the colour current are in excellent agreement for the stronger fields. This demonstrates the reliability of the TTCF approach under far-from-equilibrium conditions. However, for a weaker field (see a field of 0.001 in Figure 2), the signal-to-noise ratio becomes too small and carrying out a direct average over the 40,000 NEMD trajectories leads a very noisy and unreliable estimate for the colour conductivity. On the other hand, Figure 2 shows that the TTCF approach allows for an accurate determination of the colour conductivity for a field of 0.001. This result illustrates the inability of conventional NEMD methods to give a reliable estimate for the colour current and the colour conductivity for fields below 10^{-3} and demonstrates that the TTCF method is a definite improvement over the conventional NEMD methods.

We finally summarise the results obtained for the bulk as well as for the confined fluid for several values of the pore width in Figure 3. When the colour field tends towards zero, the value for the colour conductivity given by the TTCF approach (Equation (8)) exhibits a plateau. This is because the system enters the linear response regime as the colour field decreases. We checked for the bulk that the plateau value reached by the TTCF values for weak fields converged towards the Green–Kubo estimate for the conductivity

$$\sigma = \frac{V}{k_B T}\int_0^{\infty} \langle J_x(s)\cdot J_x(0)\rangle \mathrm{d}s. \tag{10}$$

We carried out equilibrium molecular dynamics simulations of the bulk in the NVT ensemble over 2000 time units and estimated the colour conductivity according to the following Green–Kubo expression. We found a Green–Kubo estimate for the colour conductivity of 0.048 ± 0.005. Using the TTCF approach (Equation 8), we found that the colour conductivity reached a plateau of 0.051 ± 0.005 for fields below 0.001. The excellent agreement between the Green–Kubo and the TTCF estimates is another evidence of the reliability of the TTCF approach.

As shown in Figure 3, confining the fluid in a slit nanopore systematically results in an increased conductivity with respect to the bulk. Figure 3 also shows that the conductivity strongly depends on the pore width of the nanopore. The maximum conductivity – more than twice that of the bulk – will be obtained for a pore width of about 4.

In this work, using TTCF, we showed how NEMD simulations could be extended to study the conductivity of a model liquid confined in a slit nanopore subjected to a realistic field. Our results provide a full picture of the dependence of conductivity on the applied field and on the pore width of the nanopore. Our results show that a nanoscopic confinement enhances the conductivity since

conductivity steadily increases – more than twice the value evaluated for the bulk – as the pore width decreases. The method developed in this work can be readily applied to realistic models for electrolytes for any kind of pore geometry.

References

[1] J. Petravic and J. Delhommelle, *Conductivity of molten sodium chloride and its supercritical vapor in strong dc fields*, J. Chem. Phys. 118 (2003), p. 7477.

[2] ———, *Conductivity of molten sodium chloride in an alternating electric field*, J. Chem. Phys. 119 (2003), p. 8511.

[3] W. M. Visscher, *Transport processes in solids and linear-response theory*, Phys. Rev. A 10 (1974), p. 2461.

[4] J.W. Dufty and J. Lindenfeld, *Non-linear transport in the Boltzmann limit*, J. Stat. Phys. 20 (1979), p. 259.

[5] E.G.D. Cohen, *Kinetic theory of non-equilibrium fluids*, Physica A 118 (1983), p. 17.

[6] D.J. Evans and G.P. Morriss, *Statistical mechanics of non-equilibrium liquids*, Academic Press, London, 1990.

[7] G.P. Morriss and J. Evans, *Nonlinear shear viscosity in two dimensions*, Phys. Rev. A 39 (1989), p. 6335.

[8] I. Borzsak, P.T. Cummings, and J. Evans, *Shear viscosity of a simple fluid over a wide range of strain rates*, Mol. Phys. 100 (2002), p. 2735.

[9] J. Petravic and P. Harrowell, *Linear response theory for thermal conductivity and viscosity in terms of boundary fluctuations*, Phys. Rev. E 71 (2005), p. 061201.

[10] J. Delhommelle and T. Cummings, *Simulation of friction in nanoconfined fluids for an arbitrarily low shear rate*, Phys. Rev. B 72 (2005), p. 172201.

[11] B. D. Todd, *Application of transient-time correlation functions to nonequilibrium molecular-dynamics simulations of elongational flow*, Phys. Rev. E 56 (1997), p. 6723.

[12] G. Pan, F. Ely, C. McCabe, and D.J. Isbister, *Operator splitting algorithm for isokinetic SLLOD molecular dynamics*, J. Chem. Phys. 122 (2005), p. 094114.

[13] C. Desgranges and J. Delhommelle, *Shear viscosity of liquid copper at experimentally accessible shear rates: application of the transient-time correlation function formalism*, J. Chem. Phys., in press

[14] ———, *Viscosity of liquid iron under high pressure and high temperature: equilibrium and nonequilibrium molecular dynamics simulation studies*, Phys. Rev. B 76 (2007), p. 172102.

[15] J. Delhommelle, P.T. Cummings, and J. Petravic, *Conductivity of molten sodium chloride in an arbitrarily weak dc electric field*, J. Chem. Phys. 123 (2005), p. 114505.

[16] K.P. Travis and E. Gubbins, *Poiseuille flow of Lennard-ones fluids in narrow slit pores*, J. Chem. Phys. 112 (2000), p. 1984.

[17] J. Delhommelle and J. Evans, *Configurational temperature profile in confined fluids I. Atomic fluid*, J. Chem. Phys. 114 (2001), p. 6229.

[18] ———, *Configurational temperature profile in confined fluids II. Molecular fluids*, J. Chem. Phys. 114 (2001), p. 6236.

[19] J. Delhommelle, J. Petravic, and D.J. Evans, *Reexamination of string phase and shear thickening in simple fluids*, Phys. Rev. E 68 (2003), p. 031201.

[20] ———, *On the effects of assuming the flow profile in nonequilibrium simulations*, J. Chem. Phys. 119 (2003), p. 11005.

[21] J. Delhommelle, *Should 'lane formation' occur systematically in driven liquids and colloids?*, Phys. Rev. E 71 (2005), p. 016705.

[22] ———, *Simulations of shear-induced melting in two dimensions*, Phys. Rev. B 69 (2004), p. 144117.

[23] ———, *Onset of shear-thickening in simple fluids*, Eur. Phys. J. E 15 (2004), p. 65.

[24] J. Delhommelle, J. Petravic, and D. J. Evans, *Non-newtonian behavior in simple fluids*, J. Chem. Phys. 120 (2004), p. 6117.

[25] J. Delhommelle and J. Evans, *Comparison of thermostatting mechanisms in NVT and NPT simulations of decane under shear*, J. Chem. Phys. 115 (2001), p. 43.

[26] ———, *Configurational temperature thermostat for fluids undergoing shear flow: application to liquid chlorine*, Mol. Phys. 99 (2001), p. 1825.

[27] L. Lue et al., *Configurational thermostats for molecular systems*, Mol. Phys. 100 (2002), p. 2387.

[28] J. Delhommelle and J. Evans, *Correspondence between configurational temperature and molecular kinetic temperature thermostats*, J. Chem. Phys. 117 (2002), p. 6016.

[29] J. Delhommelle and J. Petravic, *Shear viscosity of molten sodium chloride*, J. Chem. Phys. 118 (2003), p. 2783.

[30] C. Braga and P. Travis, *A configurational temperature Nosé–Hoover thermostat*, J. Chem. Phys. 123 (2005), p. 134101.

[31] H.H. Rugh, *Dynamical approach to temperature*, Phys. Rev. Lett. 78 (1997), p. 772.

[32] O.G. Jepps, G. Ayton, and D.J. Evans, *Microscopic expressions for the thermodynamic temperature*, Phys. Rev. E. 62 (2000), p. 4757.

[33] M.P. Allen and D.J. Tildesley, *Computer Simulation of Liquids*, Clarendon, Oxford, 1987.